IET Generation, Transmission & Distribution

Research Article

IET Journals
The Institution of Engineering and Technology

AC/DC multi-infeed power flow solution

ISSN 1751-8687
Received on 22nd October 2018
Revised 29th December 2018
Accepted on 4th February 2019
E-First on 18th April 2019
doi: 10.1049/iet-gtd.2018.6781
www.ietdl.org

Bilawal Rehman[1] ✉, *Chongru Liu*[1]

[1]*State Key Lab. for Alternate Electrical Power System with Renewable Energy Sources, Department of Electrical & Electronics Engineering, North China Electric Power University, Beijing, People's Republic of China*

✉ *E-mail: eer.cbr@gmail.com*

Abstract: Here, a novel approach is proposed to compute discrete value of converter tap position in AC/DC hybrid multi-infeed HVDC power flow solution. The approach is based on Newton–Raphson (NR) technique and sequential power flow method. An algorithm for the estimation of discrete tap position is devised by re-converging DC system to eliminate the error between discrete tap position and actual value of tap. The proposed technique computes new value of gamma for discrete value of tap which solves convergence problem of DC system caused by AC-voltage fluctuations. Theoretical bases and numerical results are presented to support new proposed approach. The technique is successfully applied to dual-infeed LCC HVDC feeding into the same AC system which is more practical scenario. The results validate the approach and show advantages in term of accuracy and convergence.

1 Introduction

Rapid growth of power electronics technology had made high-voltage direct current (HVDC) transmission an economic solution to transfer bulk power from generating stations to far away concentrated load areas. First point-to-point (2-terminal) HVDC link was established in 1954 between Swedish mainland and Gotland [1]. Increasing power demand enables researchers to devise topology feeding more than two terminals which initiates the concept of multi-terminal HVDC. Nowadays, a scheme termed as multi-infeed HVDC has taken much intention by seeing the exceptional growth of HVDC links for industry or bulk load in developed countries. Multi-infeed system topology consists of more than one HVDC converters feeding into the same AC system or system which lies in very close electric proximity [2–4].

Power flow analysis of hybrid integrated AC/DC system is much essential for planning new link or expansion of existing system. It also helps to investigate critical and decisive scenarios in power system which consequently cause adverse effect during abnormalities. Conventionally, Newton–Raphson (NR) power flow method is applied to solve non-linear equations of AC or AC/DC hybrid system because of its fast convergence characteristics.

Two techniques are reported in literature [5–11] to solve hybrid AC/DC power systems; (i) simultaneous and (ii) sequential. The difference between these two techniques is the way of calculation of AC/DC-integrated network equations. The simultaneous technique solves non-linear equations of both AC and DC systems simultaneously. This technique is more complex due to extended size of Jacobian matrix. It also requires to re-program the whole system because it is incapable to use existing AC power flow programmes. Moreover, it is hard to implement different power flow algorithms on both AC and DC sides. On other hand, simultaneous approach is fast and has better convergence than sequential; it also provides information about each AC/DC system. While sequential technique solves both system separately one after another. This technique has many plus points such as (i) existing AC power flow algorithm can be used; (ii) both AC and DC system may have different algorithms; (iii) it is quite easy to implement and reduces computational burden on processor; (iv) it can also provide information about each AC/DC system; and (v) separate solution of both systems reduces size of Jacobian matrix. Small size of Jacobian requires less storage and makes the technique fast. As of simple modular programming in sequential approach, various DC control modes can easily be incorporated. The sequential technique is widely used in AC/DC integrated system though it causes convergence problem in certain situations such as when DC system operates under reduced voltage level.

Fig. 1 explains simplified form of dual-infeed HVDC system. Bus 1 and bus 2 are assumed as PQ buses, while bus 3 is a slack bus. This is new topology with network impedance z_{13}, z_{23}, and z_{12} between bus 1–3, 2–3, and 1–2, respectively. The P_{di} and Q_{di} are real and reactive power, while I_{di} and U_{di} are direct current and voltage of converter i, respectively. The converter tap position and saturation reactance are denoted by T_i and X_{Ti}, while Q_{ci} denotes total reactive power supplied by installed filters and synchronous condensers or shunt capacitors at converter i.

Converter transformer tap calculations are important in HVDC control scheme with all other control parameters. Suitable tap position (T in Fig. 1) brings firing angles (α for rectifier and γ for inverter) back within range. Regardless of technique used, simultaneous or sequential as mentioned above, the key problem is to obtain appropriate tap position of converter transformer to achieve DC power balance using voltage and current characteristics.

In [9], AC–DC power flow solution of single-infeed HVDC is presented with Gauss–Seidel method using nodal analysis at each converter bus. DC systems are considered as constant current injecting to buses. However, converter tap and gamma calculations are ignored. In [10], power flow of hybrid AC/DC system is discussed with Newton trust-region method. The method uses simultaneous simplification approach to find solution. However, the tap position of converters' transformer and gamma for converters are overlooked in method. In [12], impact of control strategies is discussed for power flow of hybrid network using sequential and NR algorithms. The approach tells influence of control parameters on power flow solution of single-infeed HVDC; however, tap position and gamma values for system are missing which is practical problem of HVDCs. The load flow analysis for multi-terminal HVDC is presented in [13, 14], which incorporate converter losses with NR technique and sequential method; however, converter tap calculations are unknown for convergence. Single-infeed multiple power flow and three-level control strategies with coordination procedure is discussed in [15, 16], respectively, but the problem of discrete tap position remains unaddressed.

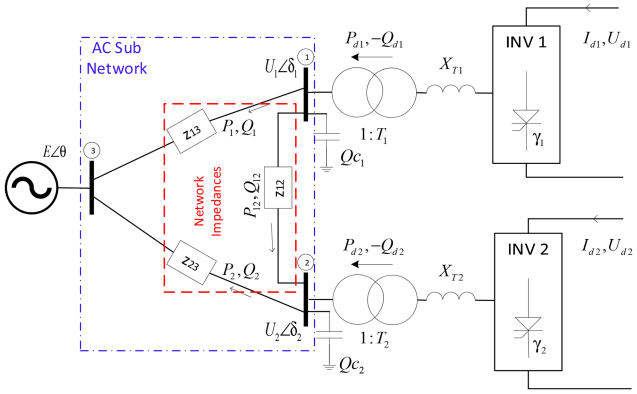

Fig. 1 *Multi-infeed HVDC system*

A detailed approach to estimate converter transformer tap position is explored in [8] using NR and sequential algorithm to solve non-linear mismatch power equations. The methodology solves convergence, imaginary reactive power, and $\cos\gamma > 1$ problem caused by voltage fluctuation at AC buses. In order to converge, converter transformer tap position is adopted as state variable instead of gamma which reveals continuous value of tap. The approach uses nearest discrete value of continuous tap to make it discrete and get proper gear number which consequently reflect error. Thus, a technique which results actual discrete value of transformer tap remains necessary and unresolved.

Here, a sequential method for power flow solution of hybrid AC/DC multi-infeed HVDC is presented. The method solves DC set of equations using interface variables computed as a result of AC system convergence. The proposed approach results actual discrete value of tap which is obtained by re-converging the whole system after selecting the discrete tap value which overcomes error caused in [8]. The approach is easy and flexible to integrate with existing AC power flow algorithms. The multi-infeed HVDC system under study is depicted in Fig. 1.

The paper is organised as: Section 2 describes AC/DC system modelling and power flow algorithm. Section 3 illustrates NR technique for AC/DC system and converter transformer tap adjustment approach. Simulation results and conclusion are presented in Sections 4 and 5, respectively.

2 Improved multi-infeed AC-DC power flow

To improve the effectiveness of sequential hybrid AC–DC power flow solution for multi-infeed HVDC, a practical, flexible, and easy technique is presented. The technique is an improved form of method discussed in [8], which has been used in China Southern Power Grid since 2007.

2.1 Algorithm formation

The algorithm to solve non-linear AC power, DC voltage, and current equations are described in this section. AC system is converged before DC based on existing multi-infeed HVDC parameters. Each HVDC in Fig. 1 is considered as load to AC system by inverting their power signs in order to simplify equations. Both converters are assumed in constant gamma control mode. The configuration used in this study is more realistic because both converters are feeding into same AC system which would reflect more practical results of multi-infeed HVDC phenomena. An overall flow chart of algorithm is shown in Fig. 2.

2.2 DC system modelling

In this study, multi-infeed (inverters) HVDC system is adopted, feeding at same AC busbar. So, in proposed approach, the gamma and converter transformer tap of each HVDC are taken as state variables. Suppose we have N AC buses and M inverters with M commutating AC sub-buses feeding at each AC bus of N. The DC voltage and current at inverter i can be expressed as (1) and (2), respectively.

$$V_{\mathrm{dc}i} = \frac{3\sqrt{2}}{\pi} B_i T_i E_{\mathrm{ac}i} \cos(\gamma_i) - \frac{3}{\pi} X_{\mathrm{Ti}} I_{\mathrm{dc}i} \tag{1}$$

$$I_{\mathrm{dc}i} = \frac{E_{\mathrm{ac}i}}{\sqrt{2} T_i X_{\mathrm{Ti}}} [\cos(\gamma_i) - \cos(\gamma_i + \mu_i)] \tag{2}$$

where B, T, γ, E_{ac}, X_T, and μ are number of bridges in each converter, converter transformer tap ratio, inverter extinction angle, AC bus voltages, transformer leakage reactance, and overlap angle, respectively. The state variable vector for DC system i is $x^i_{\mathrm{dc}} = [T_i, \gamma_i]^{\mathrm{t}}$. The t denotes transpose of vector. Similarly, the state variable vector for M inverters is as below.

$$x^{i \to M}_{\mathrm{dc}} = [T_1, T_2, \ldots, T_{M-1}, T_M, \gamma_1, \gamma_2, \ldots, \gamma_{M-1}, \gamma_M]^{\mathrm{t}}$$

The balance voltage and current equations for DC system i are

$$\begin{cases} f_{i1\mathrm{dc}} = \left[V^r_{\mathrm{dc}} - V^i_{\mathrm{dc}}(x^i_{\mathrm{dc}})\right] = 0 \\ f_{i2\mathrm{dc}} = \left[I^r_{\mathrm{dc}} - I^i_{\mathrm{dc}}(x^i_{\mathrm{dc}})\right] = 0 \end{cases} \tag{3}$$

$f_{i1\mathrm{dc}}$ and $f_{i2\mathrm{dc}}$ are functions of DC voltage and current, which reduces to 0 for x^i_{dc} while superscript r denotes required value of parameters. The mismatch vector of DC functions for M inverters will become as

$$[f_{11\mathrm{dc}}, f_{21\mathrm{dc}}, \ldots, f_{(M-1)1\mathrm{dc}}, f_{M1\mathrm{dc}}, f_{12\mathrm{dc}}, f_{22\mathrm{dc}}, \ldots, f_{(M-1)2\mathrm{dc}}, f_{M2\mathrm{dc}}]^{\mathrm{t}}$$

DC system convergence flow chart is shown in Fig. 2*a*.

2.2 AC system modelling

The voltage magnitude and angle of AC buses are chosen as state variables. The real and reactive power at inverter commutating bus j for AC sub-network in Fig. 1 can be expressed as (4) and (5), respectively. Here, $j = 1, 2, \ldots, M$.

$$P_j = \sum_{w=1}^{M+1} |V_j|\,|V_w|\,|Y_{\mathrm{jw}}| \cos(\theta_{\mathrm{jw}} - \delta_j + \delta_w) \tag{4}$$

$$Q_j = -\sum_{w=1}^{M+1} |V_j|\,|V_w|\,|Y_{\mathrm{jw}}| \sin(\theta_{\mathrm{jw}} - \delta_j + \delta_w) \tag{5}$$

$|V_j|$, $|Y_{\mathrm{jw}}|$, θ_{jw}, and δ_j are voltage magnitude, magnitude of element of admittance matrix, angle of element of admittance matrix, and bus voltage angle, respectively. The state variable vector for converter j commutating AC bus is $x^j_{\mathrm{ac}} = [\delta_j, |V_j|]^{\mathrm{t}}$. Similarly, the state variable vector for AC commutating buses having M inverters is

$$x^{j \to M}_{\mathrm{ac}} = [\delta_1, \delta_2, \ldots, \delta_{(M-1)}, \delta_M, |V_1|, |V_2|, \ldots, |V_{(M-1)}|, |V_M|]^{\mathrm{t}}$$

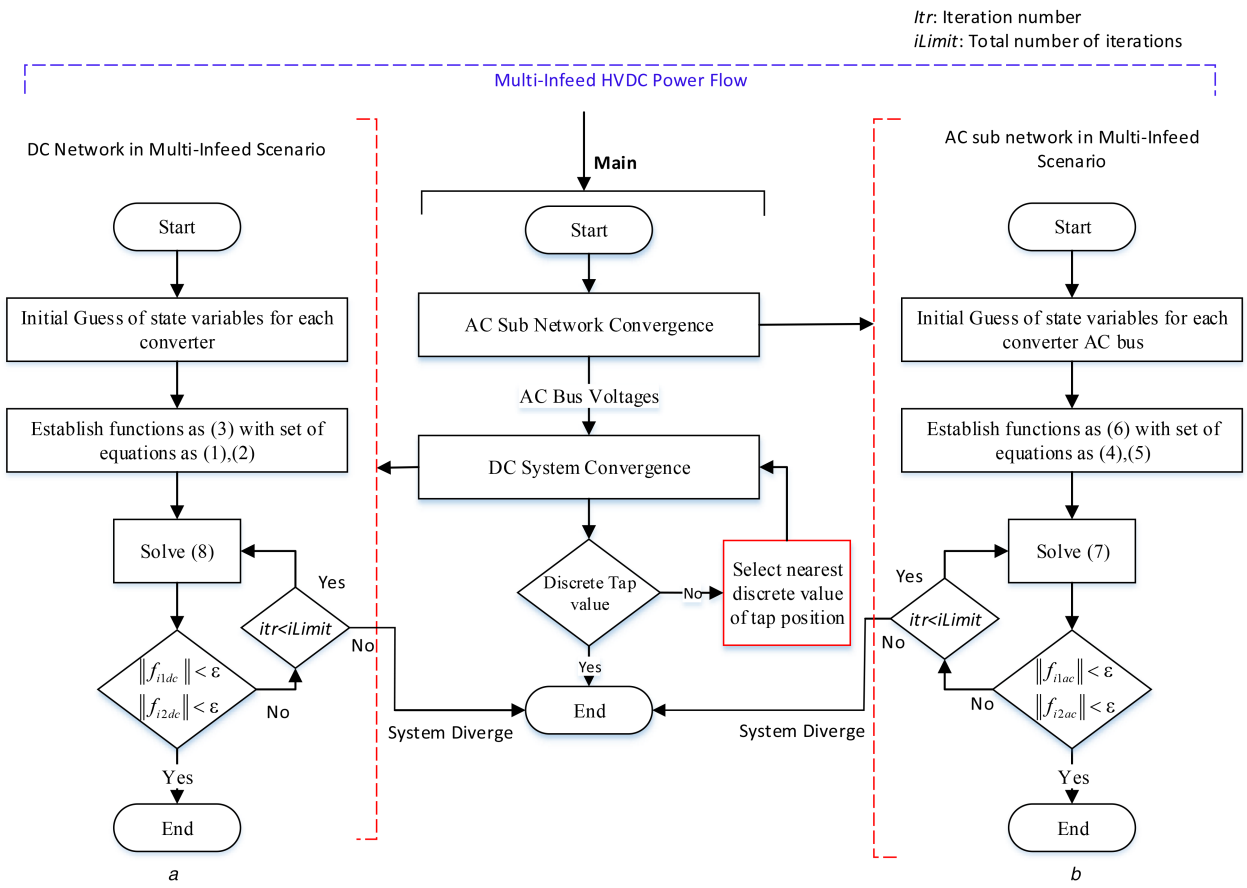

Fig. 2 *Overall flow chart of power flow convergence of multi-infeed HVDC*
(a) DC Network, ***(b)*** AC sub network

The mismatch real and reactive power equations at converter j commutation bus are

$$\begin{cases} f_{j1\text{ac}} = \left[P_j^r - P_j(x_{\text{ac}}^j)\right] = 0 \\ f_{j2\text{ac}} = \left[Q_j^r - Q_j(x_{\text{ac}}^j)\right] = 0 \end{cases} \tag{6}$$

$f_{j1\text{ac}}$ and $f_{j2\text{ac}}$ are functions of P and Q which reduces to 0 for x_{ac}^j. The vector of mismatch functions for AC sub-system having M inverters is as

$$[f_{11\text{ac}}, f_{21\text{ac}}, \ldots, f_{(M-1)1\text{ac}}, f_{M1\text{ac}}, f_{12\text{ac}}, f_{22\text{ac}}, \ldots f_{(M-1)2\text{ac}}, f_{M2\text{ac}}]^{\text{t}}$$

AC sub-network convergence flow chart is illustrated in Fig. 2*b*.

3 Newton–Raphson solution

In this work, NR method with sequential algorithm is applied for multi-infeed HVDC. AC sub-network is converged first to get bus voltage magnitude for DC system. The AC/DC system having two inverters and two commutating AC buses can be solved by NR method as (7) and (8) for state variables.

Equations (7) and (8) are solved iteratively with prescribed tolerance to get converged solution of system.

$$\begin{bmatrix} f_{11\text{ac}}^{(k)} \\ f_{21\text{ac}}^{(k)} \\ f_{12\text{ac}}^{(k)} \\ f_{22\text{ac}}^{(k)} \end{bmatrix} = \begin{bmatrix} \frac{\partial P_1^{(k)}}{\partial \delta_1} & \frac{\partial P_1^{(k)}}{\partial \delta_2} & \frac{\partial P_1^{(k)}}{\partial |V_1|} & \frac{\partial P_1^{(k)}}{\partial |V_2|} \\ \frac{\partial P_2^{(k)}}{\partial \delta_1} & \frac{\partial P_2^{(k)}}{\partial \delta_2} & \frac{\partial P_2^{(k)}}{\partial |V_1|} & \frac{\partial P_2^{(k)}}{\partial |V_2|} \\ \frac{\partial Q_1^{(k)}}{\partial \delta_1} & \frac{\partial Q_1^{(k)}}{\partial \delta_2} & \frac{\partial Q_1^{(k)}}{\partial |V_1|} & \frac{\partial Q_1^{(k)}}{\partial |V_2|} \\ \frac{\partial Q_2^{(k)}}{\partial \delta_1} & \frac{\partial Q_2^{(k)}}{\partial \delta_2} & \frac{\partial Q_2^{(k)}}{\partial |V_1|} & \frac{\partial Q_2^{(k)}}{\partial |V_2|} \end{bmatrix} \begin{bmatrix} \delta_1^{(k)} \\ \delta_2^{(k)} \\ |V_1^{(k)}| \\ |V_2^{(k)}| \end{bmatrix} \tag{7}$$

$$\begin{bmatrix} f_{11\text{dc}}^{(k)} \\ f_{21\text{dc}}^{(k)} \\ f_{12\text{dc}}^{(k)} \\ f_{22\text{dc}}^{(k)} \end{bmatrix} = \begin{bmatrix} \frac{\partial V_{\text{dc1}}^{(k)}}{\partial T_1} & 0 & \frac{\partial V_{\text{dc1}}^{(k)}}{\partial \gamma_1} & 0 \\ 0 & \frac{\partial V_{\text{dc2}}^{(k)}}{\partial T_2} & 0 & \frac{\partial V_{\text{dc2}}^{(k)}}{\partial \gamma_2} \\ \frac{\partial I_{\text{dc1}}^{(k)}}{\partial T_1} & 0 & \frac{\partial I_{\text{dc1}}^{(k)}}{\partial \gamma_1} & 0 \\ 0 & \frac{\partial I_{\text{dc2}}^{(k)}}{\partial T_2} & 0 & \frac{\partial I_{\text{dc2}}^{(k)}}{\partial \gamma_2} \end{bmatrix} \begin{bmatrix} T_1^{(k)} \\ T_2^{(k)} \\ \gamma_1^{(k)} \\ \gamma_2^{(k)} \end{bmatrix} \tag{8}$$

3.1 Tap adjustment

Literature shows two methods to deal converter tap position [5, 8, 17–19]: (i) fix tap position to a preset value and (ii) move tap position 1 gear for each iteration. Consequently, AC/DC power flow convergence might need long iterations, exhibit error or even fail due to incorrect tap position. This paper proposes a new method to get discrete tap position for converter transformer as follows: (i) AC sub-system is converged first to get bus voltages for DC system with existing network impedances and HVDC parameters (7), (ii) DC system with AC bus voltages is converged with (8) to get tap position value and gamma of each converter, (iii) tap position is set to nearest discrete value and (iv) DC system is again converged with discrete tap value in step 3 and AC bus voltages from step 1 to get new value of gamma and to eradicate error. A process flow chart is provided below (Fig. 3) to elaborate complete steps.

3.2 DC power calculation

The algorithm convergence flow chart of AC/DC hybrid multi-infeed HVDC is shown in Fig. 2. The proposed approach adjusts transformer tap position in normal and contingency situations such as DC system operates under voltage or reduced power. After

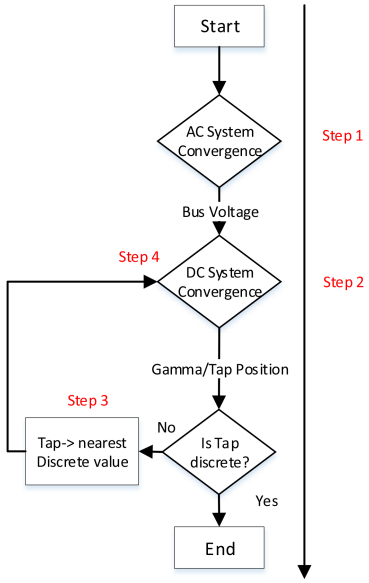

Fig. 3 *Process flow chart of complete procedure*

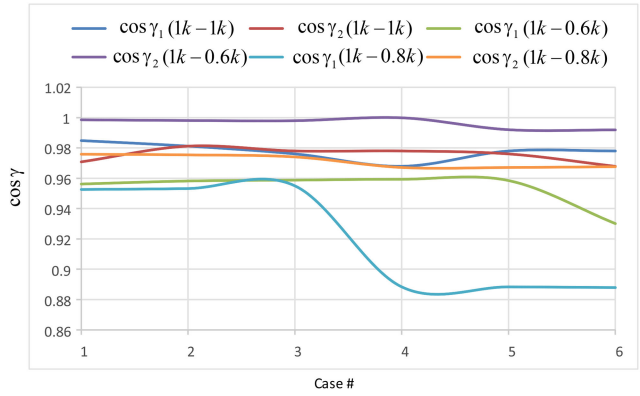

Fig. 4 *Behaviour of cos γ versus case number (next section)*

convergence of DC converter i, the DC active and reactive powers can be calculated as (9) and (10), respectively.

$$P_{\mathrm{dc}}^{i} = V_{\mathrm{dc}}^{i} I_{\mathrm{dc}}^{i} \tag{9}$$

$$Q_{\mathrm{dc}}^{i} = I_{\mathrm{dc}}^{i} \sqrt{\left(V_{\mathrm{dc0}}^{i}\right)^{2} - \left(V_{\mathrm{dc}}^{i}\right)^{2}} \tag{10}$$

The values of cos γ is provided in Fig. 4 for few cases (discussed in next section). Fig. 4 proves that cos γ is always <1 for more practical and variable AC bus voltages at each converter with proposed power flow solution, which authenticates the method presented here. Moreover, if cos $\gamma < 1$ then (1) yields (11); subsequently, (10) forbids imaginary reactive power problem because $\left(\left(V_{\mathrm{dc0}}^{i}\right)^{2} - \left(V_{\mathrm{dc}}^{i}\right)^{2}\right) > 1$.

$$\begin{cases} V_{\mathrm{dc0}i} > V_{\mathrm{dc}i} + \dfrac{3}{\pi} X_{Ti} I_{\mathrm{dc}i} > V_{\mathrm{dc}i} \\ V_{\mathrm{dc0}i} = \dfrac{3\sqrt{2}}{\pi} B_i T_i E_{\mathrm{ac}i} \end{cases} \tag{11}$$

Thus, imaginary reactive power, cos γ, and convergence problem with discrete tap position can easily be solved with technique described here. Furthermore, the approach requires very less number of iterations compared to techniques presented in the literature.

4 Simulation

The set of equations described here are properly modelled in order to verify the results. AC sub-system of multi-infeed HVDC (as in Fig. 1) has network impedances (z_{13}, z_{23} and z_{12}); thus, there are numerous results to proposed approach. The network impedances are kept constant during power flow solution and selected in such a way that AC/DC system works in stable region (positive eigenvalues i.e. $\lambda_{\min} > 0$). For example, $z_{13} = 2.5$ p.u., $z_{23} = 2.5$ p.u., and $z_{12} = 20$ p.u. produce minimum eigenvalue of 0.323. The proposed approach is verified with dual-infeed HVDC with three sets of converter ratings; (i) (1k–1k) MW, (ii) (1k–0.6k) MW, and (iii) (1k–0.8k) MW each with 500 kV. The values of other parameters such as slack bus voltages, transformer leakage reactance, number of bridges, and overlap angle are 1.05 p.u., 0.18 p.u., 2, 0.209 radian, respectively. In proposed approach, ±16 gears with step size of 0.040 are chosen, which ranges between 0.36 and 1.64. Tables 1 and 2 illustrate calculations of AC sub-system and DC state variables with given network impedances for set 1. The corrected gamma with discrete tap position is also tabulated. The k_{ac} and k_{dc} are number of iterations for AC and DC systems, respectively. The state variables for both AC and DC dual-infeed HVDC system with set 2 are given in Tables 3 and 4. The set 3 is also investigated, and the results are provided in Tables 5 and 6.

Fig. 5 shows error caused by rounding off converter tap position (T) to nearest discrete value for proper adjustment of gear number. However, this rounding off also produces error in γ as illustrated in Fig. 5. The gamma readjustment technique presented here eradicates this error and significantly affects overall reactive power consumption, stability sensitivity, maximum achievable power, and power flow studies.

4.1 IEEE 14 bus system with HVDC

To verify the proposed scheme, IEEE 14 bus system with parameters in CIGRE brochure [20] is modelled with HVDC_1 connected at bus 10 and HVDC_2 connected at bus 11 (see Fig. 6). The power signs are reversed in order to attach HVDC systems as load i.e. $(-P_1, Q_1)$ and $(-P_2, Q_2)$. Several simulations are performed with different power ratings and the results are tabulated below (Table 7). The error columns validate that the scheme can reduce error in extinction angle, while selecting the discrete tap position.

The tabulated results clearly show the validity of technique presented. Thus, the calculation error occurred due to regulation of continues tap position to nearest discrete value can be prevented by approach described here.

5 Conclusion

This paper proposes an improved technique to estimate discrete converter tap position and gamma with the help of sequential and

Table 1 Dual-infeed (1000–1000 MW) – AC system convergence results

Case	z_{13}	z_{23}	z_{12}	$\|V_1\|$	$\|V_2\|$	δ_1	δ_2	k_{ac}
1	2.0	3.5	20	1.390	1.267	1.222	1.717	2
2	2.5	2.5	20	1.352	1.352	1.400	1.400	2
3	3.0	2.5	20	1.305	1.321	1.570	1.532	2
4	3.5	2.5	20	1.248	1.322	1.588	1.699	2
5	2.5	3.0	20	1.321	1.305	1.532	1.570	2
6	2.5	3.5	20	1.322	1.248	1.699	1.588	2

Table 2 Dual-infeed (1000–1000 MW) – DC system convergence results

Case	k_{dc}	γ_1	γ_2	T_1	T_2	γ_1^{new}	γ_2^{new}	T_1^{new}	T_2^{new}
1	5	0.176	0.240	0.316	0.352	0.174	0.242	0.360	0.360
2	5	0.194	0.194	0.327	0.327	0.194	0.194	0.360	0.360
3	5	0.218	0.209	0.340	0.335	0.219	0.210	0.360	0.360
4	5	0.253	0.209	0.359	0.335	0.254	0.210	0.360	0.360
5	5	0.209	0.218	0.335	0.340	0.210	0.219	0.360	0.360
6	5	0.209	0.253	0.335	0.359	0.210	0.254	0.360	0.360

Table 3 Dual-infeed (1000–600 MW) – AC system convergence results

Case	z_{13}	z_{23}	z_{12}	$\|V_1\|$	$\|V_2\|$	δ_1	δ_2	k_{ac}
1	2.5	3.5	20	1.181	1.318	1.153	0.424	2
2	2.5	3.5	25	1.191	1.302	1.124	0.487	2
3	2.5	3.5	30	1.195	1.295	1.113	0.513	2
4	2.5	3.1	40	1.198	1.418	1.107	0.266	2
5	2.5	4.0	40	1.192	1.172	1.113	0.750	2
6	2.8	4.0	40	1.104	1.147	1.264	0.791	2

Table 4 Dual-infeed (1000–600 MW) – DC system convergence results

Case	k_{dc}	γ_1	γ_2	T_1	T_2	γ_1^{new}	γ_2^{new}	T_1^{new}	T_2^{new}
1	5	0.303	0.068	0.384	0.310	0.297	0.053	0.400	0.360
2	5	0.294	0.072	0.380	0.314	0.290	0.061	0.400	0.360
3	5	0.291	0.074	0.378	0.316	0.288	0.063	0.360	0.360
4	5	0.288	0.044	0.377	0.288	0.286	0.012	0.360	0.360
5	4	0.293	0.115	0.380	0.350	0.289	0.126	0.400	0.360
6	4	0.380	0.125	0.423	0.358	0.376	0.127	0.440	0.360

Table 5 Dual-infeed (1000–800 MW) – AC system convergence results

Case	z_{13}	z_{23}	z_{12}	$\|V_1\|$	$\|V_2\|$	δ_1	δ_2	k_{ac}
1	2.5	3.0	20	1.164	1.165	1.180	0.489	2
2	2.5	3.0	21	1.167	1.162	1.172	0.501	2
3	2.5	3.0	25	1.174	1.152	1.150	0.532	2
4	3.0	3.0	25	1.035	1.093	1.342	0.634	2
5	3.0	3.0	27	1.035	1.094	1.342	0.634	2
6	3.0	3.0	30	1.034	1.096	1.342	0.634	2

Table 6 Dual-infeed (1000–800 MW) – DC system convergence results

Case	k_{dc}	γ_1	γ_2	T_1	T_2	γ_1^{new}	γ_2^{new}	T_1^{new}	T_2^{new}
1	3	0.318	0.209	0.392	0.369	0.309	0.220	0.400	0.360
2	3	0.315	0.211	0.391	0.370	0.307	0.222	0.400	0.360
3	3	0.309	0.217	0.387	0.374	0.301	0.228	0.400	0.360
4	3	0.486	0.258	0.474	0.398	0.477	0.257	0.480	0.400
5	3	0.487	0.257	0.474	0.397	0.477	0.257	0.480	0.400
6	3	0.488	0.256	0.474	0.397	0.478	0.255	0.480	0.400

NR convergence algorithm. Conventionally, converter discrete tap position is being obtained by rounding off continuous tap position to nearest discrete value. However, this process produces error in converter gamma value which subsequently affects maximum achievable power, total reactive power consumption, and power flow studies. The technique presented here for multi-infeed scenario eradicates error in gamma produced by tap position by re-converging DC system to find new value of gamma after selecting the discrete tap value. The approach is easy and flexible to integrate with existing AC power flow algorithms. It also forbids

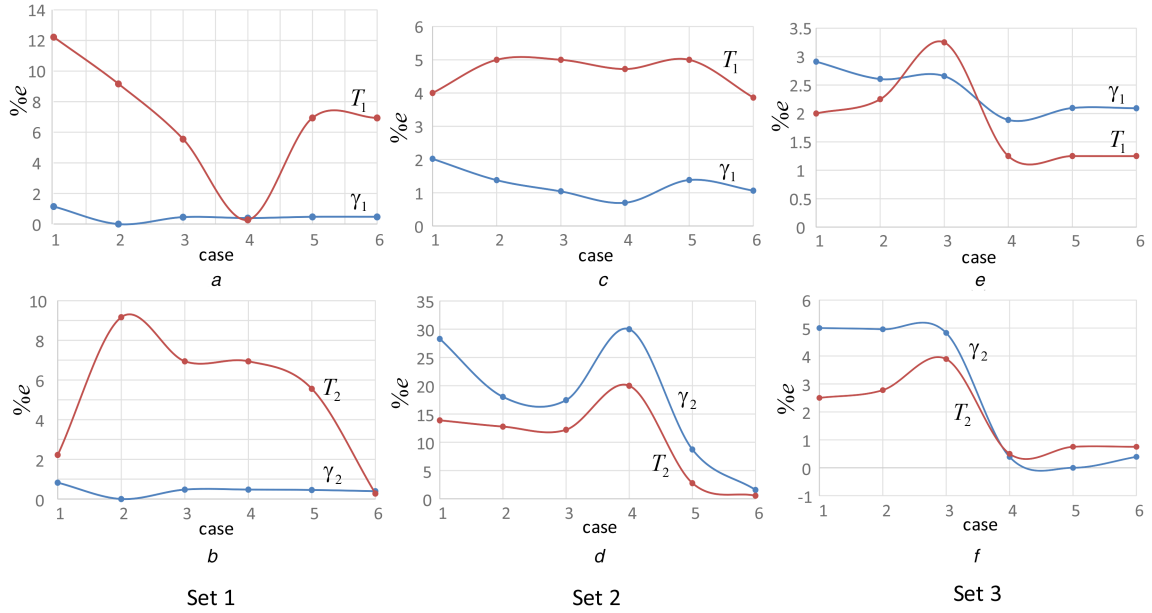

Fig. 5 *Percentage error in converter γ and T by rounding off T to nearest discrete tap position for 3 sets of dual-infeed HVDC system; set 1(a&b), set 2(c&d) and set 3(e&f)*

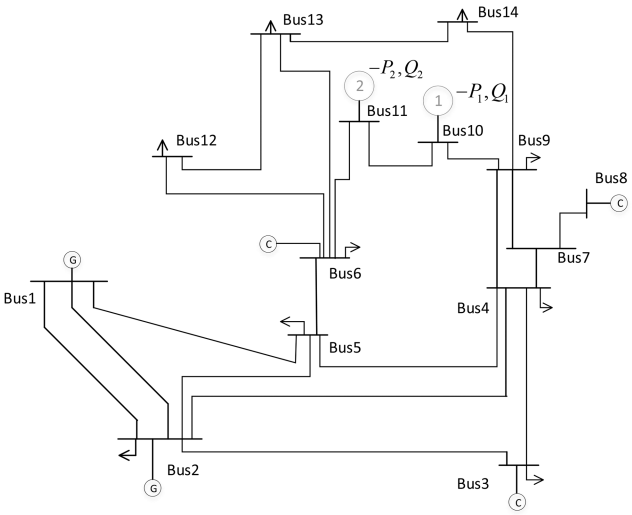

Fig. 6 *IEEE 14 Bus system with HVDC systems attached at bus 10 and 11*

Table 7 IEEE 14 bus system with HVDC results

P_1	P_2	γ_1	γ_2	T_1	T_2	γ_{1new}	γ_{2new}	T_{1new}	T_{2new}	%e γ_1	%e γ_1	%eT_1	%eT_2
1000	1000	0.543	0.54	0.501	0.508	0.536	0.553	0.52	0.52	1.306	2.351	3.654	2.308
1000	800	0.528	0.562	0.498	0.504	0.54	0.543	0.48	0.52	2.222	3.499	3.750	3.077
1000	600	0.531	0.551	0.497	0.503	0.539	0.539	0.48	0.52	1.484	2.226	3.542	3.269
800	600	0.523	0.53	0.495	0.497	0.532	0.538	0.48	0.48	1.692	1.487	3.125	3.542
800	300	0.479	0.564	0.476	0.511	0.488	0.557	0.48	0.52	1.844	1.257	0.833	1.731

impractical situations such as convergence, imaginary reactive power, and power flow oscillation problems. The improved approach is applied on various scenarios having dual-infeed LCC HVDC feeding into same AC system. The theoretical analysis and numerical simulation results illustrate that the method has advantages to previous techniques.

6 References

[1] Rodriguez, P., Rouzbehi, K.: 'Multi-terminal DC grids: challenges and prospects', *J. Mod. Power Syst. Clean Energy*, 2017, **5**, (4), pp. 515–523

[2] Aik, D.L.H., Andersson, G.: 'Voltage stability analysis of multi-infeed HVDC systems', *IEEE Trans. Power Deliv.*, 1997, **12**, (3), pp. 1309–1318

[3] Lee, D.H.A., Andersson, G.: 'An equivalent single-infeed model of multi-infeed HVDC systems for voltage and power stability analysis', *IEEE Trans. Power Deliv.*, 2016, **31**, (1), pp. 303–312

[4] Hau Aik, D.L., Anderson, G.: 'Power stability analysis of multi-infeed HVDC systems', *IEEE Trans. Power Deliv.*, 1998, **13**, (3), pp. 923–931

[5] Sheblc, G.B., Member, S., Grigsby, L.L., *et al.*: 'A new approach to AC/DC power flow', *IEEE Trans. Power Syst.*, 1991, **6**, (3), pp. 1238–1244

[6] Reeve, J., Fahny, G., Stott, B.: 'Versatile load flow method for multiterminal HVDC systems', *IEEE Trans. Power Appar. Syst.*, 1977, **96**, (3), pp. 925–933

[7] Fudeh, H., Ong, C.M.: 'A simple and efficient AC–DC load-flow method for multiterminal DC systems', *IEEE Trans. Power Appar. Syst.*, 1981, **PAS-100**, (11), pp. 4389–4396

[8] Liu, C., Zhang, B., Hou, Y., *et al.*: 'An improved approach for AC–DC power flow calculation with multi-infeed DC systems', *IEEE Trans. Power Syst.*, 2011, **26**, (2), pp. 862–869

[9] Yalcin, F., Arifoglu, U.: 'A new sequential AC–DC power flow algorithm for multi-terminal HVDC systems', *IEEJ Trans. Electr. Electron. Eng.*, 2017, **12**, pp. 65–71

[10] Eajal, A.A., Abdelwahed, M.A., El-Saadany, E.F., *et al.*: 'A unified approach to the power flow analysis of AC/DC hybrid microgrids', *IEEE Trans. Sustain. Energy*, 2016, **7**, (3), pp. 1145–1158

[11] Hamad, A.A., Member, S., Azzouz, M.A., *et al.*: 'A sequential power flow algorithm for islanded hybrid AC/DC microgrids', *IEEE Trans. Power Syst.*, 2016, **31**, (5), pp. 3961–3970
[12] Khan, S., Bhowmick, S.: 'Impact of DC link control strategies on the power-flow convergence of integrated AC–DC systems', *Ain Shams Eng. J.*, 2016, **7**, (1), pp. 249–264
[13] Khan, M., Zaman, S., Noh, C.-H., *et al.*: 'A load flow analysis for AC/DC hybrid distribution network incorporated with distributed energy resources for different grid scenarios', *Energies*, 2018, **11**, (2), p. 367
[14] Jef Beerten, R.B., Cole, S.: 'A sequential AC/DC power flow algorithm for networks containing multi-terminal VSC HVDC systems'. IEEE PES General Meeting, Providence, RI, USA, 2010, pp. 1–7
[15] Fan, Y.K., Niebur, D., Nwankpa, C.O., *et al.*: 'Multiple power flow solutions of small integrated AC/DC power systems'. IEEE Int. Symp. Circuits and Systems, Geneva, Switzerland, 2000, pp. 224–227
[16] Liu, C., Bose, A., Han, M., *et al.*: 'Improved continuation power flow method for AC/DC power system'. IEEE Electrical Power and Energy Conf., Winnipeg, MB, Canada, 2011, pp. 192–198
[17] Thukaram, D., Yesuratnam, G.: 'Optimal reactive power dispatch in a large power system with AC–DC and FACTS controllers', *IET Gener. Transm. Distrib.*, 2008, **2**, (1), pp. 71–81
[18] Yang, Z., Zhong, H., Bose, A., *et al.*: 'Optimal power flow in AC–DC grids with discrete control devices', *IEEE Trans. Power Syst.*, 2018, **33**, (2), pp. 1461–1472
[19] Cañizares, C.A., Alvarado, F.L.: 'Point of collapse and continuation methods for large AC/DC systems', *IEEE Trans. Power Syst.*, 1993, **8**, (1), pp. 1–8
[20] PSCAD: IEEE 14 Bus System, Revision 1 (https://hvdc.ca/knowledge-base/read,article/26/ieee-14-bus-system/v:). Winnipeg, Manitoba: Manitoba Hyro International, 2018.